Polyhedron 52 (2013) 1306–1316

Contents lists available at SciVerse ScienceDirect

Polyhedron

journal homepage: www.elsevier.com/locate/poly

Different geometries of novel cobalt(II) compounds with 2-hydroxy-benzophenones and neocuproine: Crystal and molecular structures of [Co(2-hydroxy-benzophenone)$_2$(neoc)], [Co(2-hydroxy-4-methoxybenzophenone)(neoc)Br] and [Co(neoc)Br$_2$]·CH$_3$OH·H$_2$O

Maria Lalia-Kantouri [a,*], Christos D. Papadopoulos [a], Antonios G. Hatzidimitriou [a], Michael P. Sigalas [b], Miguel Quirós [c], Stavroula Skoulika [d]

[a] Aristotle University of Thessaloniki, Department of Chemistry, Laboratory of Inorganic Chemistry, Thessaloniki 54 124, Greece
[b] Aristotle University of Thessaloniki, Department of Chemistry, Laboratory of Applied Quantum Chemistry, Thessaloniki 54 124, Greece
[c] University of Granada, Department of Inorganic Chemistry, Faculty of Science, Granada 18071, Spain
[d] University of Ioannina, Department of Chemistry, Laboratory of Physical Chemistry, Ioannina, Greece

ARTICLE INFO

Article history:
Available online 15 June 2012

Dedicated to Alfred Werner on the 100th Anniversary of his Nobel Prize in Chemistry in 1913.

Keywords:
Cobalt
2-Hydroxy-benzophenones
Neocuproine
DFT study
Thermal study
Crystal structures

ABSTRACT

Ten mixed-ligand Co(II) compounds with 2-hydroxy-benzophenones(ketones) and neocuproine(neoc) were synthesized and characterized by physicochemical and spectral (IR, UV–Vis) data. The cyclic voltammetry study in CH$_3$CN gave all the expected waves for the redox processes of the metal Co(II) and the studied ligands. The X-ray diffraction study of two representative compounds proved the two different geometries, octahedral for [Co(2-hydroxy-benzophenone)$_2$(neoc)] (**3**) and trigonal bipyramidal for [Co(2-hydroxy-4-methoxybenzophenone)(neoc)Br] (**10**). Additionally, the precursor compound [Co(neoc)Br$_2$]·CH$_3$OH·H$_2$O (**11**) was proved by (X-ray) to posses tetrahedral geometry. The molecular structure and the possible isomers of the trigonal bipyramidal complex **10** were studied by means of density functional calculations (DFT). The thermal stability was investigated by means of simultaneous TG/DTG–DTA technique in nitrogen atmosphere up to 1000 °C, where metallic cobalt was found as the solid residue.

1. Introduction

Both 1,10-phenanthrolines and 2,2′-bipyridines are attractive building blocks in organic chemistry, strongly chelating for a variety of metal ions [1]. Metal-ion complexes with functionalized 1,10-phenanthrolines and 2,2′-bipyridines have been used as catalyst for the enantioselective hydrolysis of N-protected amino acid esters [2], in the oxidative cleavage of DNA [3] and in palladium catalyzed allylic substitution [4]. Specifically, cobalt chelates with 2,2′-bipyridine (bipy) or 1,10-phenanthroline (phen) possess various geometries forming cationic octahedral complexes, e.g. [Co(bipy)$_3$]$^{2+}$ and [Co(phen)$_3$]$^{2+}$ [5], which are known to have important biological properties [6], or neutral octahedral complexes of the type [Co(bipy)$_2$Br$_2$] and [Co(phen)$_2$Br$_2$], or even cationic square-pyramidal complexes of the type [Co(bipy)$_2$Br]$^+$. In the case, however, of cobalt chelates with 2,9-dimethyl-1,10-phenanthroline (neocuproine, neoc) there is a pronounced reduction in coordination geometry at the metal center, from octahedral in solution, [Co(neoc)(H$_2$O)$_4$]$^{2+}$ to tetrahedral in solid state, [Co(neoc)(SiO)$_2$]$^{2+}$ and [Co(neoc)(SCN)$_2$] [7] or [Co(neoc)Br$_2$] in this work.

Besides, the strong coordinating properties of 2-hydroxy-benzophenones or 2-hydroxy-benzaldehydes (salicylaldehyde, saloH) and their derivatives with 3d transition metals have stimulated research in these compounds, which find applications in both pure [8] and applied chemistry fields, especially in extractive metallurgy as analytical reagents [9,10] and specifically for cobalt compounds in tyre industry as adhesion promoters [11]. These ligands are known to coordinate in a bidentate manner with transition metals in the mono-anionic form, adopting square-planar geometry, [Zn(salo)$_2$], [Zn-5-Br-salo] [12], [Cu(5-Br-salo)$_2$] [13], [Fe^{II}(salo)$_2$] [14] or octahedral arrangement [VO(3-OCH$_3$-salo)$_2$(H$_2$O)] [15], [Fe^{III}(2-hydroxy-propiophenone)$_3$] [16].

For a better understanding of the bonds and properties in these compounds we have initiated a research project with the metals cobalt and iron and ligands with N and/or O donor atoms. The

---

* Corresponding author. Tel./fax: +30 2310 997844.
E-mail addresses: lalia@chem.auth.gr (M. Lalia-Kantouri), hatzidim@chem.auth.gr (A.G. Hatzidimitriou), sigalas@chem.auth.gr (M.P. Sigalas), mquiros@ugr.es (M. Quirós), vskoul@uoi.gr (S. Skoulika).

0277-5387/$ - see front matter © 2012 Elsevier Ltd. All rights reserved.
http://dx.doi.org/10.1016/j.poly.2012.06.012

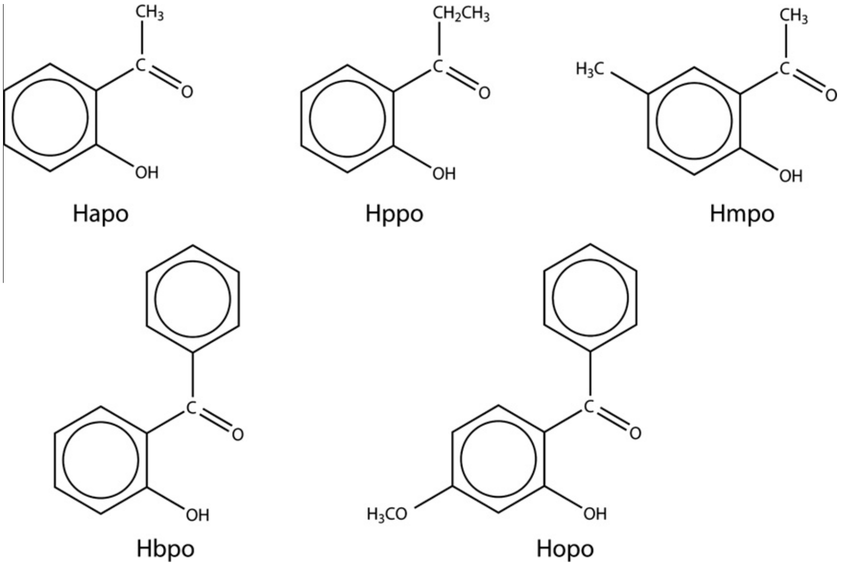

Scheme 1. Structural formulae of the 2-hydroxy-phenone ligands.

Lewis acidity of [Co^{II}(salo)$_2$] chelates, renders them susceptible to nucleophilic attack and addition compounds can be obtained, such as [Co(salo)$_2$(α-diimines)] (where α-diimines are bipy, phen or neoc) [17,18]. Recently, from the reaction of the precursor compound [Co(bipy)$_2$Br$_2$] or [Co(phen)$_2$Br$_2$] with the anion of a 2-hydroxy-phenone ligand(keto), the addition compounds with octahedral geometry [Co^{II}(keto)$_2$(bipy)]·Hketo or [Co^{II}(keto)$_2$(phen)] have been obtained [19].

Continuing our research, we present here the results of the reaction of the precursor compound [Co(neoc)Br$_2$] with the anion of a 2-hydroxy-benzophenone ligand(keto). This reaction led to the formation and isolation of two groups of neutral cobalt(II) compounds with two different geometries each one, depending on the metal-to-ligand stoichiometric ratio. The crystal and molecular structures of two representative compounds, each one from the two groups, as well as of the precursor compound were verified by X-ray diffraction analysis. The thermal stability and decomposition mode for three of the new compounds were studied in nitrogen atmosphere by using the simultaneous technique (TG/DTG–DTA). Results of density functional (DFT) calculations for compound [Co(opo)(neoc)Br] were used to explore the possibility for the compound to adopt different conformations.

The 2-OH-benzophenones presented in this work have the molecular formula 2-OH-$C_6H_4C(R)O$, where R = CH_3, C_2H_5 or C_6H_5, commonly known and abbreviated as 2-OH-acetophenone(Hapo) (**1**′), 2-OH-propiophenone(Hppo) (**2**′), 2-OH-benzophenone(Hbpo) (**3**′), respectively, as well as their derivatives 2-OH, 5-CH_3-acetophenone(Hmpo) (**4**′) and 2-OH, 4-OCH_3-benzophenone(Hopo) (**5**′), (Scheme 1).

2. Experimental

2.1. Materials

The ligands, 2-hydroxy-phenones (**1**′–**5**′), the 2,9-dimethyl-1,10-phenanthroline, neocuproine, abbreviated as neoc), and the metal salt $CoBr_2{\cdot}6H_2O$ were obtained as reagent grade from Aldrich and used as received. Solvents for preparation and physical measurements of “extra pure” grade were obtained from Fluka without further purification.

2.2. Instrumentation/analytical procedures

Microanalyses were carried out using a Perkin-Elmer 240 B CHN microanalyzer and Perkin-Elmer 5100 PC Atomic Absorption Spectrophotometer for the metal content. Infrared spectra were recorded on a Perkin-Elmer 1600 FT-IR spectrometer in KBr discs at room temperature and are reported in cm^{-1}. Electronic absorption spectra in CH_3CN solutions were obtained on a Shimatzu 160 A spectrometer. Molar conductivities were measured in CH_3CN solutions, employing a WTW conductivity bridge and a calibrated dip type cell. Magnetic susceptibility measurements on powdered samples were performed at 25 °C employing the Faraday method on a home-build balance calibrated against Hg[Co(SCN)$_4$].

Cyclic voltammetry technique (CV) was used for the electrochemical measurements on a μ-AUTOLAB Potentio-Galvanostat (ECO CHEMIE, Netherlands). A saturated calomel electrode was used as a reference electrode and a platinum plate one as an auxiliary electrode for all measurements. As a working electrode a platinum wire was used. The tests in CH_3CN solution were carried out in the potential region −1900 to +2200 mV at ambient temperature. Recrystallized TEA perchlorate 0.1 M was used as the electrolyte at a scan rate 100 mV/s. All scans were recorded in degassed solvent, under current of moisture free argon over the solution surface. The thermal behavior of the title compounds was studied in nitrogen using the simultaneous TG/DTG–DTA technique, over the temperature range ambient-to-980 °C, using a Setaram Model Setsys-1200 thermogravimetric analyzer. The samples, with a mass of about 12 mg were heated in platinum crucibles, at a heating rate 5 and/or 10 °C/min.

2.2.1. Computational details

The electronic structure and geometries of the complexes studied were computed within the density functional theory (DFT) using gradient corrected functional, at the Becke3LYP computational level [20,21]. The effective core potential (ECP) approximation of Hay and Wadt was used [22–24]. For Co atom, the electrons described by the ECP were those of 1s, 2s and 2p shells. The basis set used was of valence double-ζ quality [25]. Full geometry optimizations were carried out without symmetry constraints. A frequency calculation after each geometry optimization ensured that the calculated structures are real minima or transition states in the potential energy surface of the molecules and allowed the calculation of the zero point energy. All the calculations were performed using the GAUSSIAN-03W version 6.0 package [26].

2.3. X-ray structural determination

Crystals for compounds [Co(bpo)$_2$(neoc)] (**3**) (orange-brownish) and [Co(opo)(neoc)Br] (**10**) (dark-green) were obtained from the reaction mixture after slow evaporation. Crystals (green-blue bars) of the precursor [Co(neoc)Br$_2$]·CH$_3$OH·H$_2$O (**11**), suitable for X-ray, were prepared by recrystallization from methanol. Crystals of compound **3** were mounted on a Brucker P4 diffractometer employing Mo Kα radiation. The data collection was accomplished by operating the diffractometer in the xscan mode using the scintillation method at ambient temperature. Crystals of compound **10** were mounted on a Bruker SMART APEX CCD system with Mo Kα radiation (λ = 0.71073 Å). The data collection was accomplished by operating the diffractometer in the ϕ and ω scans mode modes at ambient temperature. Crystals of compound **11** were mounted on a CAD4 automatic diffractometer employing Mo Kα radiation. The lattice parameters were calculated by least squares refinement of 25 strong reflections ($17° < \theta < 19°$) which were specifically measured for this purpose. The collection of the reflections was accomplished by operating the diffractometer in the ω/2θ scan mode at ambient temperature.

All crystals were air and beam stable during the data collection. The point group's determination was followed by the position determination of the non hydrogen atoms using SUPERFLIP program [27] for **11** and SHELXS-97 [28a] for compounds **3** and **10**. Subsequent calculations and data refinement were finalized using SHELXL-97 [28b] for **3** and **10** and CRYSTALS version 12.83 [29] for compound **11**. All hydrogen atoms were revealed to be at their expected positions. All those belonging to the ligands except them of the methyl group were positioned geometrically, while the rest were refined using soft restraints on the bond lengths and angles to regularize their geometry (C–H bonds and angles to 1.00 (Å) and 109 (°), and O–H bonds to 0.90 (Å), angles to 109 (°)). After the non hydrogen atoms anisotropic refinement, all hydrogen atoms positions were refined with riding constraints. A summary of the crystallographic data is listed in Table 1.

2.4. General procedure for the preparation of the cobalt(II) compounds

2.4.1. Preparation of the compounds [Co(2-OH-benzophenone)$_2$(neoc)] (*1–5*)

All complexes have been prepared by the following general procedure. A solution of 1 mmol 2-hydroxy-benzophenone and CH$_3$O-Na (1 mmol) in MeOH (30 mL), was added drop-wise to a solution of [Co(neoc)Br$_2$] (0.5 mmol) in H$_2$O (20 mL) at room temperature, according to the reaction:

$$[\mathrm{Co(neoc)Br_2}] + 2\mathrm{ketoH} + 2\mathrm{CH_3ONa} \rightarrow [\mathrm{Co(keto)_2(neoc)}] + 2\mathrm{NaBr} + 2\mathrm{CH_3OH}$$

The solution was stirred for 2 h and then turned darker and an orange-brownish solid was formed. The solid was filtered, washed with water and dried in vacuo (mean yield 62%). All compounds were prepared in inert, under argon, conditions and well degassed solutions have been used.

*2.4.1.1. Synthesis of [Co(apo)$_2$(neoc)] (**1**).* The compound was prepared according to the general procedure by employing 2-OH-acetophenone(Hapo) (136 mg, 1 mmol) and CH$_3$ONa (54 mg, 1 mmol) in MeOH (25 mL), to [Co(neoc)Br$_2$] (0.214 g, 0.5 mmol) in H$_2$O (20 mL) at room temperature, under argon atmosphere. The

Table 1
Crystal data and structure refinements for compounds [Co(bpo)$_2$(neoc)] (**3**), [Co(opo)(neoc)Br] (**10**) and [Co(neoc)Br$_2$]·CH$_3$OH·H$_2$O (**11**).

	3	**10**	**11**
Empirical formula	$C_{40}H_{30}CoN_2O_4$	$C_{28}H_{23}BrCoN_2O_3$	$C_{15}H_{18}Br_2Co_1N_2O_2$
Formula weight (g mol)	661.59	574.32	477.06
λ (Å)	0.71073	0.71073	0.71073
Crystal system	monoclinic	monoclinic	monoclinic
Space group	$P2_1/c$	$P2_1/n$	$P2_1/n$
Unit cell dimensions			
a (Å)	11.3689(17)	9.658(2)	7.933(5)
b (Å)	16.701(2)	23.556(3)	13.123(7)
c (Å)	17.007(3)	11.002(1)	18.211(9)
β (°)	92.090(3)	100.97(1)	101.96(2)
V (Å^3)	3226.9(8)	2457.3(6)	1854.7(18)
Z	4	4	4
Calculated density (mg m^{-3})	1.362	1.552	1.708
Absorption coefficient (mm^{-1})	0.577	2.358	5.240
$F(000)$	1372	1164	940
Crystal size (mm)	0.49 × 0.24 × 0.22	0.13 × 0.11 × 0.10	0.19 × 0.20 × 0.27
θ range for data collection (°)	1.71–28.38	2.07–25.00	1.93–25.67
Limiting indices	$-13 \leqslant h \leqslant 15, -21 \leqslant k \leqslant 20, -21 \leqslant l \leqslant 20$	$0 \leqslant h \leqslant 11, -1 \leqslant k \leqslant 28, -13 \leqslant l \leqslant 12$	$-9 \leqslant h \leqslant 9, 0 \leqslant k \leqslant 16, 0 \leqslant l \leqslant 22$
Reflections observed/unique	20209/7408 (R(int) = 0.0327)	4760/4301 (R(int) = 0.0265)	5082/3522 (R(int) = 0.021)
Completeness	99.0% to θ = 25.58	99.4% to θ_{max}	99.9% to θ_{max}
Refinement method	Full-matrix least-squares on F^2	Full-matrix least-squares on F^2	Full-matrix least-squares on F^2
Weighting scheme	$w = 1/[\sigma^2(F_o^2)+(0.07P)^2 + 0.7P]$ where $P = (F_o^2 + 2F_c^2)/3$	$w = 1/[\sigma^2(F_o^2)+(0.0532P)^2 + 5.8035P]$ where $P = (F_o^2 + 2F_c^2)/3$	$w = 1/[\sigma^2(F^2) + (0.07P)^2 + 1.03P]$ where $P = (\max(F_o^2,0) + 2F_c^2)/3$
Data/parameters	7408/426	4301/316	3486/199
Goodness-of-fit on F^2	1.037	1.056	1.010
R_1, wR_2 [$I > 2\sigma(I)$]	0.0550, 0.1283	0.0454, 0.1151	0.0310, 0.0680
R_1, wR_2 (all data)	0.0733, 0.1380	0.0722, 0.1325	0.0356, 0.0704
Largest difference in peak/hole (e Å^{-3})	0.607/−0.277	0.509/−0.512	0.48/−0.57

crystalline orange-brownish compound (0.17 g, 61% yield), analyzed as *Anal.* Calc. for $C_{30}H_{28}N_2O_5Co_1$ (MW 537): C, 67.06; H, 4.84; N, 5.21; Co, 10.98. Found: C, 66.85; H, 4.82; N, 5.12; Co, 10.75%. Magnetic value ($\mu_{eff} = 4.10\ \mu_B$), conductivity in freshly prepared CH_3CN solutions (9.2 μS/cm). IR spectrum (KBr): selected peaks in cm^{-1}: 1604 vs 1590 vs 1361 s, 859 m, 731 s, 552 m, 454 m. UV–Vis bands in nm: 345, 400(sh), 660, 995.

*2.4.1.2. Synthesis of [Co(ppo)$_2$(neoc)] (**2**).* The compound was prepared according to the general procedure by employing 2-OH-propiophenone(Hppo) (150 mg, 1 mmol) and CH_3ONa (54 mg, 1 mmol) in MeOH (25 mL), to [Co(neoc)Br_2] (0.214 g, 0.5 mmol) in H_2O (20 mL). The crystalline orange-brownish compound (0.20 g, 71% yield), analyzed as *Anal.* Calc. for $C_{32}H_{30}N_2O_4Co_1$ (MW 565): C, 67.96; H, 5.30; N, 4.95; Co, 10.44. Found: C, 68,04; H, 5.26; N, 4.87; Co, 10.50%. Magnetic value ($\mu_{eff} = 4.08\ \mu_B$), conductivity in CH_3CN 7.12 μS/cm. IR spectrum (KBr): selected peaks in cm^{-1}: 1611 vs 1594 vs 1376 s, 861 m, 732 s, 552 m, 450 m. UV–Vis bands in nm: 345, 402(sh), 663, 995.

*2.4.1.3. Synthesis of [Co(bpo)$_2$(neoc)] (**3**).* The compound was prepared according to the general procedure by employing 2-OH-benzophenone(Hbpo) (198 mg, 1 mmol) and CH_3ONa (54 mg, 1 mmol) in MeOH (25 mL), to [Co(neoc)Br_2] (0.214 g, 0.5 mmol) in H_2O (15 mL) The crystalline compound (0.17 g, 51% yield), analyzed as *Anal.* Calc. for $C_{40}H_{30}N_2O_4Co_1$ (MW 661): C, 71.33; H, 4.59; N, 4.33; Co, 8.92. Found: C, 72.62; H, 4.54; N, 4.23; Co, 8.97%. Magnetic value ($\mu_{eff} = 4.15\ \mu_B$), conductivity in CH_3CN 6.43 μS/cm. IR spectrum (KBr): selected peaks in cm^{-1}: 1603 vs 1587 vs 1354 s, 854 m, 759 s, 592 m, 411 m. UV–Vis bands in nm: 345, 400(sh), 670, 990.

*2.4.1.4. Synthesis of [Co(mpo)$_2$(neoc)] (**4**).* The compound was prepared according to the general procedure by employing 2-OH, 5-CH_3-acetophenone(Hmpo) (150 mg, 1 mmol) and CH_3ONa (54 mg, 1 mmol) in MeOH (25 mL), to [Co(neoc)Br_2] (0.214 g, 0.5 mmol) in H_2O (15 mL). The crystalline compound (0.19 g, 67% yield), analyzed as *Anal.* Calc. for $C_{32}H_{30}N_2O_4Co_1$ (MW 565): C, 67.96; H, 5.31; N, 4.95; Co, 10.44. Found: C, 68.03; H, 5.40; N, 4.87; Co, 10.40%. Magnetic value ($\mu_{eff} = 4.12\ \mu_B$), conductivity in CH_3CN 5.7 μS/cm. IR spectrum (KBr): selected peaks in cm^{-1}: 1605 vs 1594 vs 1359 s, 856 m, 730 s, 551 m, 401. UV–Vis bands in nm: 345, 405(sh), 660, 998.

*2.4.1.5. Synthesis of [Co(opo)$_2$(neoc)] (**5**).* The compound was prepared according to the general procedure by employing 2-OH, 4-OCH_3-benzophenone(Hopo) (228 mg, 1 mmol) and CH_3ONa (54 mg, 1 mmol) in MeOH (25 mL), to [Co(neoc)Br_2] (0.214 g, 0.5 mmol) in H_2O (15 mL). The crystalline compound (0.21 g, 58% yield), analyzed as *Anal.* Calc. for $C_{42}H_{34}N_2O_6Co_1$ (MW 721): C, 69.90; H, 4.71; N, 3.88; Co, 8.18. Found: C, 69.54; H, 4.80; N, 3.91; Co, 8.20%. Magnetic value ($\mu_{eff} = 4.30\ \mu_B$), conductivity in CH_3CN 8.7 μS/cm. IR spectrum (KBr): selected peaks in cm^{-1}: 1604 vs 1584 vs 1371 s, 857 m, 730 s, 549 m, 418 m. UV–Vis bands in nm: 343, 402(sh), 670, 992.

2.4.2. Preparation of the compounds [Co(2-OH-benzophenone)(neoc)Br] (6–10)

All complexes have been prepared by the following general procedure. A solution of 0.5 mmol 2-hydroxy-benzophenone and CH_3ONa (0.5 mmol) in MeOH (20 mL), was added drop-wise to a solution of [Co(neoc)Br_2] (0.5 mmol) in H_2O (20 mL) at room temperature, according to the reaction:

$$[\mathrm{Co(neoc)Br_2}] + \mathrm{ketoH} + \mathrm{CH_3ONa} \rightarrow [\mathrm{Co(keto)(neoc)Br}] + \mathrm{NaBr} + \mathrm{CH_3OH}$$

The solution was stirred for 2 h and then turned darker and a dark-greenish solid was formed. The solid was filtered, washed with water and dried in vacuum (mean yield 56%). All compounds were prepared in inert, under argon, conditions and well degassed solutions have been used.

*2.4.2.1. Synthesis of [Co(apo)(neoc)Br] (**6**).* The compound was prepared according to the general procedure by employing 2-OH-acetophenone(Hapo) (136 mg, 1 mmol) and CH_3ONa (54 mg, 1 mmol) in MeOH (25 mL), to [Co(neoc)Br_2] (0.427 g, 1 mmol) in H_2O (20 mL). The dark-green crystalline compound (0.26 g, 52% yield), analyzed as *Anal.* Calc. for $C_{22}H_{21}Br_1N_2O_3Co_1$ (MW 482): C, 54.77; H, 3.94; N, 5.81; Co, 12.24. Found: C, 54.44; H, 3.90; N, 5.68; Co, 12.08%. Magnetic value ($\mu_{eff} = 4.20\ \mu_B$), conductivity in freshly prepared CH_3CN solutions (9.3 μS/cm), IR spectrum (KBr): selected peaks in cm^{-1}: 1601 vs 1581 vs 1363 s, 860 m, 733 s, 565 m, 430 m, 303 m, 215 w. UV–Vis bands in nm: 325, 420(sh), 520, 590.

*2.4.2.2. Synthesis of [Co(ppo)(neoc)Br] (**7**).* The compound was prepared according to the general procedure by employing 2-OH-propiophenone(Hppo) (150 mg, 1 mmol) and CH_3ONa (54 mg, 1 mmol) in MeOH (25 mL), to [Co(neoc)Br_2] (0.427 g, 1 mmol) in H_2O (20 mL). The dark-green crystalline compound (0.29 g, 58% yield), analyzed as *Anal.* Calc. for $C_{23}H_{21}Br_1N_2O_2Co_1$ (MW 496): C, 55.64; H, 4.23; N, 5.64; Co, 11.89. Found: C, 55,10; H, 4.78; N, 5.58; Co, 11.84%. Magnetic value ($\mu_{eff} = 4.22\ \mu_B$), conductivity in CH_3CN 8.20 μS/cm. IR spectrum (KBr): selected peaks in cm^{-1}: 1609 vs 1588 vs 1372 s, 855 m, 745 s, 560 m, 415 m, 301 m, 215 w. UV–Vis bands in nm: 318, 420(sh), 525, 595.

*2.4.2.3. Synthesis of [Co(bpo)(neoc)Br] (**8**).* The compound was prepared according to the general procedure by employing 2-OH-benzophenone(Hbpo) (198 mg, 1 mmol) and CH_3ONa (54 mg, 1 mmol) in MeOH (25 mL), to [Co(neoc)Br_2] (0.427 g, 1 mmol) in H_2O (20 mL). The dark-green crystalline compound (0.27 g, 50% yield), analyzed as *Anal.* Calc. for $C_{27}H_{21}Br_1N_2O_2Co_1$ (MW 544): C, 59.56; H, 3.86; N, 5.14; Co, 10.84. Found: C, 59.61; H, 3.91; N, 5.32; Co, 10.80%. Magnetic value ($\mu_{eff} = 4.29\ \mu_B$), conductivity in CH_3CN 9.50 μS/cm. IR spectrum (KBr): selected peaks in cm^{-1}: 1602 vs 1582 vs 1351 s, 850 m, 731 s, 550 m, 417 m, 305 m, 218 w. UV–Vis bands in nm: 320, 418(sh), 520, 590.

*2.4.2.4. Synthesis of [Co(mpo)(neoc)Br] (**9**).* The compound was prepared according to the general procedure by employing 2-OH, 5-CH_3-acetophenone(Hmpo) (150 mg, 1 mmol) and CH_3ONa (54 mg, 1 mmol) in MeOH (25 mL), to [Co(neoc)Br_2] (0.427 g, 1 mmol) in H_2O (20 mL). The crystalline compound (0.32 g, 65% yield), analyzed as *Anal.* Calc. for $C_{23}H_{21}Br_1N_2O_2Co_1$ (MW 496): C, 55.65; H, 4.23; N, 5.64; Co, 11.89. Found: C, 55.82; H, 4.84; N, 5.30; Co, 11.85%. Magnetic value ($\mu_{eff} = 4.19\ \mu_B$), conductivity in CH_3CN 8.6 μS/cm. IR spectrum (KBr): selected peaks in cm^{-1}: 1603 vs 1590 vs 1360 s, 853 m, 731 s, 560 m, 420, 303 m, 216 w. UV–Vis bands in nm: 325, 412(sh), 522, 593.

*2.4.2.5. Synthesis of [Co(opo)(neoc)Br] (**10**).* The compound was prepared according to the general procedure by employing 2-OH, 4-OCH_3-benzophenone(Hopo) (228 mg, 1 mmol) and CH_3ONa (54 mg, 1 mmol) in MeOH (25 mL), to [Co(neoc)Br_2] (0.427 g, 1 mmol) in H_2O (20 mL). The crystalline compound (0.31 g, 54% yield), analyzed as *Anal.* Calc. for $C_{28}H_{23}Br_1N_2O_3Co_1$ (MW 574): C, 58.53; H, 4.00; N, 4.87; Co, 10.27. Found: C, 58.56; H, 4.05; N, 4.91; Co, 10.25%. Magnetic value ($\mu_{eff} = 4.17\ \mu_B$), conductivity in CH_3CN 7.6 μS/cm. IR spectrum (KBr): selected peaks in cm^{-1}: 1606 vs 1584 vs 1368 s, 855 m, 733 s, 550 m, 417 m, 303 m, 217 w. UV–Vis bands in nm: 320, 420(sh), 520, 590.

2.4.3. Synthesis of the precursor compound [Co(neoc)Br_2]·CH_3OH·H_2O (**11**)

The precursor compound [Co(neoc)Br_2] was prepared according to known procedure [30,18], by reacting $CoBr_2$ with neocuproine in a metal to ligand ratio 1:2, in CH_3CN solution and reflux for 2 h under argon atmosphere. Air stable green-blue crystals, suitable for X-ray collected after 5 days by recrystallization from methanol.

3. Results and discussion

3.1. Synthesis and characterization

The reaction of the precursor compound [Co(neoc)Br_2] with the anion of a 2-OH-phenone ligand (keto), under proper inert conditions, led to the formation of two groups of cobalt(II) compounds with two different geometries each one, depending on the metal-to-ligand stoichiometric ratio. Thus, 1 mmol of a deprotonated substituted 2-OH-phenone ligand reacted with 0.5 mmol of [Co(neoc)Br_2] under argon (1:2 ratio) to give five microcrystalline orange-brown products of the first group. The elemental analyses and the absence of electrical conductivity in CH_3CN solutions indicated neutral adduct compounds, with the general formulae [Co(keto)$_2$(neoc)] (**1**–**5**). When, however, 1 mmol of a deprotonated substituted 2-OH-phenone ligand reacted with 1 mmol of [Co(neoc)Br_2] under argon (1:1 ratio) the products formed were five deep-green microcrystalline solids belonging to the second group. The elemental analyses and the absence of electrical conductivity in CH_3CN solutions indicated neutral mixed-ligand complexes with the general formulae [Co(keto)(neoc)Br] (**6**–**10**).

All new compounds are stable in air, soluble in almost all the organic solvents, but insoluble in diethylether and water. The experimental magnetic moments at room temperature for the studied compounds of both groups (mean value $\mu_{\text{eff}} = \sim 4.2\ \mu_B$) corroborate with high-spin Co(II) complexes, in accordance with other analogous compounds [31,32].

The coordination mode of the ligands in the new cobalt compounds was examined using spectroscopic methods (IR and electronic excitation (UV–Vis) spectra). The X-ray crystallographic analysis for two of them (one compound from each group, that is [Co(bpo)$_2$(neoc)] (**3**) and [Co(opo)(neoc)Br] (**10**)) provided evidence regarding the different geometry around cobalt(II) ion and the configuration of the ligands. Moreover, X-ray study of the precursor compound [Co(neoc)Br_2)]·CH_3OH·H_2O (**11**), proved this to possess a tetrahedral geometry with the bromide ions coordinated to the cobalt atom.

3.2. Description of the structures

Compounds [Co(bpo)$_2$(neoc)] (**3**) and [Co(opo)(neoc)Br] (**10**) crystallize in the Monoclinic crystal system with space groups $P2_1/c$ and $P2_1/n$, respectively. Figs. 1 and 2 depict the clinographic projection of the molecules, with displacement ellipsoids drawn at the 50% probability level, produced with the CAMERON program [33], while selected distances (Å) and bond angles (°) are given in Tables 2 and 3.

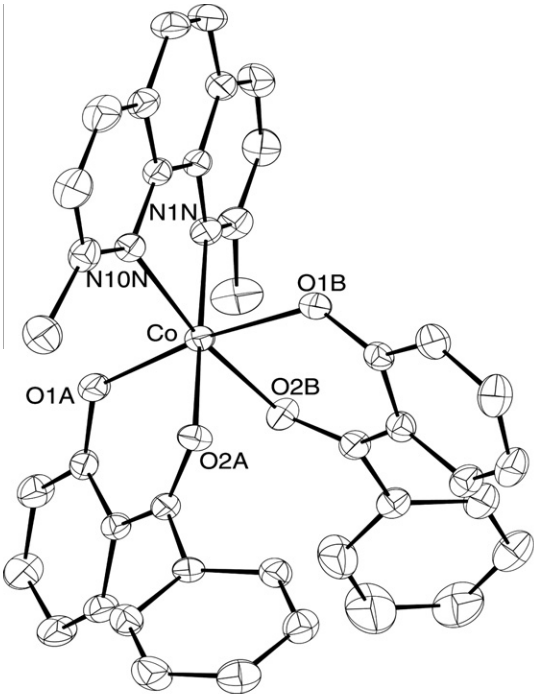

Fig. 1. Clinographic projection of [Co(bpo)$_2$(neoc)] (**3**) with displacement ellipsoids drawn at the 50% probability level. Hydrogen atoms have been omitted.

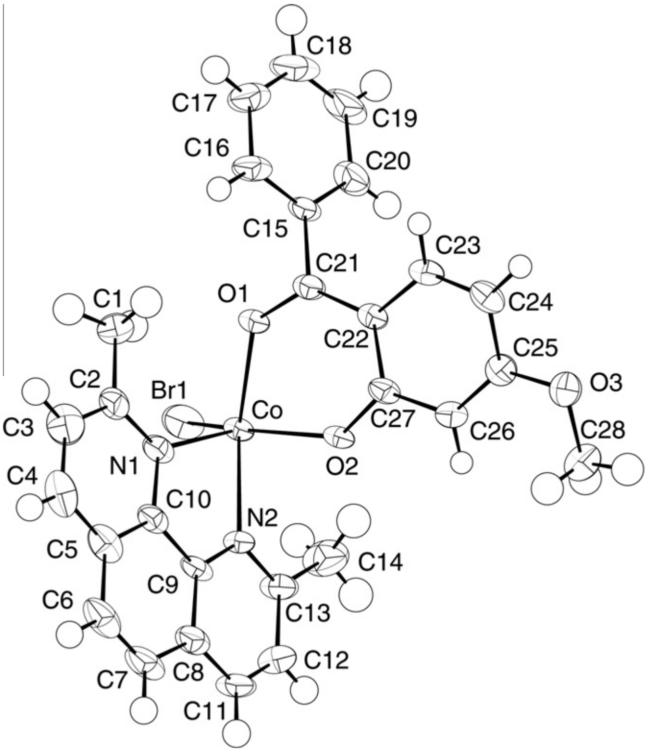

Fig. 2. Clinographic projection of [Co(opo)(neoc)Br] (**10**) with displacement ellipsoids drawn at the 50% probability level.

In both compounds **3** and **10** the cobalt atom is coordinated to the 2-OH-benzophenone and neocuproine ligands in a bidendate mode. The compounds exhibit different coordination geometries since in the structure of **3** the coordination number is six, while in the case of **10** the coordination number is five. In the unit cell of compound **3**, [Co(bpo)$_2$(neoc)] four neutral complexes can be found. These four molecules are arranged in a way that, π−π interactions between the delocalized π electronic systems coming from the neocuproine ligands of neighboring molecules, are stacking them together. These considerably strong interactions are keeping the neocuproine ligands in a parallel arrangement at distances of 3.34 Å. The molecular structure (Fig. 1) reveals a distorted octahedral coordination symmetry around the metal ion with the most axial vector passing through O(2A), Co and N(1N). If O(2A) and N(1N) would be considered to occupy the axial positions, then O(1A), O(1B), N(10N) and O(2B) form the equatorial coordination

Table 2
Selected bond lengths (Å) and angles (°) for **3**.

Co–O(1A)	1.9749(17)
Co–O(1B)	2.0278(17)
Co–O(2A)	2.0971(17)
Co–O(2B)	2.1101(17)
Co–N(1N)	2.176(2)
Co–N(10N)	2.179(2)
O(1A)–Co–O(1B)	171.23(7)
O(1A)–Co–O(2A)	85.61(7)
O(1B)–Co–O(2A)	87.86(7)
O(1A)–Co–O(2B)	89.82(7)
O(1B)–Co–O(2B)	83.73(7)
O(2A)–Co–O(2B)	84.52(7)
O(1A)–Co–N(1N)	96.91(7)
O(1B)–Co–N(1N)	89.88(7)
O(2A)–Co–N(1N)	176.47(7)
O(2B)–Co–N(1N)	97.94(7)
O(1A)–Co–N(10N)	97.33(7)
O(1B)–Co–N(10N)	89.61(7)
O(2A)–Co–N(10N)	100.57(7)
O(2B)–Co–N(10N)	171.49(7)
N(1N)–Co–N(10N)	76.69(8)

Table 3
Selected bond lengths (Å) and angles (°) for **10**.

Co–O(2)	1.972(3)
Co–O(1)	2.068(4)
Co–N(1)	2.109(4)
Co–N(2)	2.141(4)
Br(1)–Co	2.4562(10)
O(2)–Co–O(1)	86.08(14)
O(2)–Co–N(1)	121.63(16)
O(1)–Co–N(1)	104.66(16)
O(2)–Co–N(2)	84.86(15)
O(1)–Co–N(2)	170.67(15)
N(1)–Co–N(2)	78.40(17)
O(2)–Co–Br(1)	129.81(12)
O(1)–Co–Br(1)	92.11(11)
N(1)–Co–Br(1)	107.34(11)
N(2)–Co–Br(1)	95.38(12)

plane. All coordination distances and angles are similar with those reported in analogous complexes [19,34]. The atoms forming the equatorial plane present a maximum deviation 0.102(14) Å from it (for O(2B)), while the Co(II) cation was found to be 0.003(15) Å lower of the plane (with a deviation smaller than the error). The neocuproine moiety was found to be practically planar with deviations smaller or equal than the error as well as the phenyl rings of the 2-OH-benzophenone ligands. The dihedral angle between the mean equatorial plane and the neocuproine ligand was found to be 71.98°. The dihedral angles formed between the phenyl rings of each 2-OH-benzophenone ligand with the equatorial plane were 54.23° and 67.89°.

The crystal structure of **10**, [Co(opo)(neoc)Br] contains four mononuclear neutral Co(II) complex moieties present in the unit cell. Each mononuclear complex moiety (Fig. 2) is strongly interacting with two neighboring molecules with strong $\pi-\pi$ interactions. These are arising from the neocuproine delocalized π system to the same system from a neighboring molecule, with the two systems being virtually parallel and lying at a distance of 3.29 Å. The same π system is also interacting with the phenyl ring of an another neighboring complex moiety being almost planar to it, with an angle of 8.11° and in a distance of 3.36 Å, as shown in Fig. 3.

The molecular structure of compound **10** (Fig. 2) consists from a metal cation bonded to one 2-OH-benzophenone and one neocuproine ligand, both in a chelate bidentate mode. The five-membered metal coordination sphere is accomplished by one bromine atom. The bond distances and the bite angles of both the organic ligands are similar to those found at other analogous cobalt complexes [35a,35b].

The bond distances and angles of the coordinated atoms (Table 2) as well as the *tau* value proposed from Addison et al. [36], could led us to propose trigonal bipyramidal geometry for the five-membered coordination sphere around cobalt. Generally $\tau = (\beta - \alpha)/60$ and values close to zero indicate square-based pyramidal geometry while values close to one indicate trigonal bypiramidal geometry. In our case, as α and β are the values of the angles N(2)–Co–O(1) = 170.67 and N(1)–Co–Br(1) = 107.34, respectively, $\tau = 1.0555$, value very close to one and the geometry around cobalt could be virtually considered as trigonal bipyramidal.

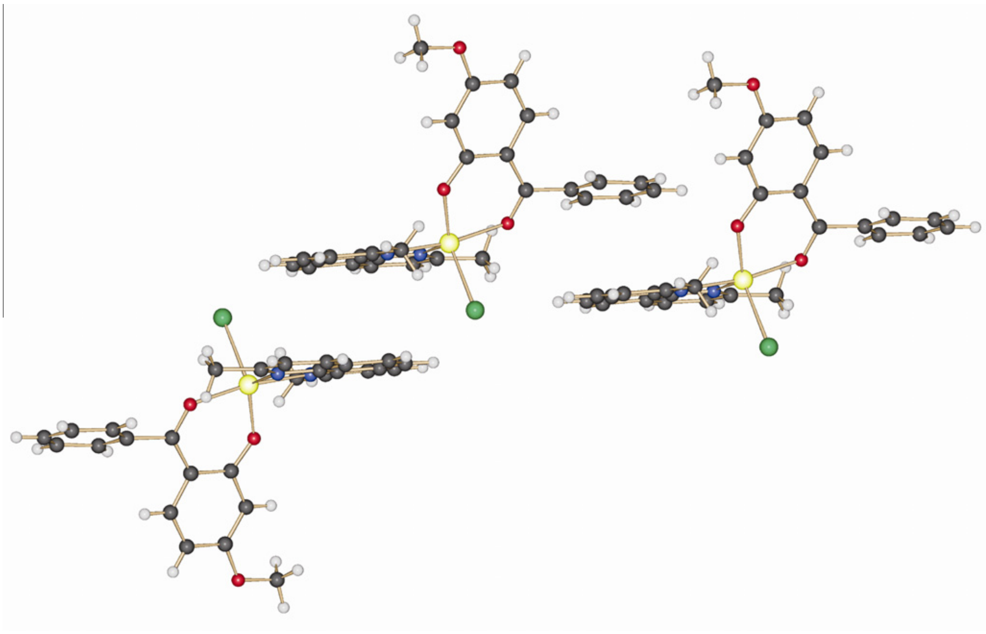

Fig. 3. Projection along *c* axis of a part of the structure of compound **10** presenting the two types of intra molecular $\pi-\pi$ aromatic interactions.

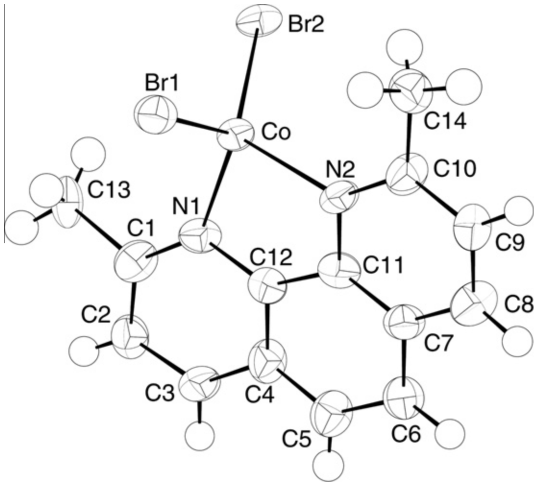

Fig. 4. Clinographic projection of the precursor [Co(neoc)Br_2]·CH_3OH·H_2O (**11**) with displacement ellipsoids drawn at the 50% probability level. Solvent molecules have been omitted.

Table 4
Selected bond lengths (Å) and angles (°) for **11**.

Br(1)–Co(1)	2.3981(14)
Br(2)–Co(1)	2.3948(12)
Co(1)–N(1)	2.047(3)
Co(1)–N(2)	2.028(3)
Br(1)–Co–Br(2)	118.28(4)
Br(1)–Co–N(1)	113.39(10)
Br(2)–Co–N(1)	111.02(11)
Br(1)–Co–N(2)	112.72(11)
Br(2)–Co–N(2)	110.80(11)
N(1)–Co–N(2)	86.23(15)

The trigonal bipyramidal base is formed from N(1), O(2) and Br(1) atoms while the axial positions are occupied from O(1) and N(2). The atoms forming the mean basal plane belong on it, while the cobalt atom is placed 0.136(4) Å upper this and the O(1) atom further upper at 2.165(4) Å, while N(2) is placed 1.970(4) Å lower. The neocuproine ligand is practically planar forming an angle of 78.08° with the equatorial plane. The dihedral angle formed between the phenyl rings of the 2-OH-benzophenone ligand was 63.90°.

Compound [Co(neoc)Br_2]·CH_3OH·H_2O (**11**) crystallizes in the $P2_1/n$ space group with four formula units in the unit cell. Fig. 4 depicts the clinographic projection of the molecule, while selected distances (Å) and bond angles (°) are given in Table 4.

The molecular structure of the precursor compound (**11**) is quite simple. The central Co(II) metal ion is coordinated to the two nitrogen atoms of the neocuproine ligand and to two bromine atoms in a tetrahedral mode. All coordination distances and bond angles are similar to those found in similar compounds [37]. The crystal structure of the compound consist from four complex moieties arranged as the previous compounds, but with very light interactions between neighboring parallel neocuproine ligands at distances of 3.87 Å. A strong local hydrogen bonding net between the water molecule, the methanol molecule and the coordinated bromine anions is present with O(water)–Br mean distances of 3.05 Å and O(water)–O(methanol) distance of 2.64(1) Å.

3.3. Computational studies using DFT

The molecular structure of complex [Co(opo)(neoc)Br] (**10**) in its quadruple ground state was optimized under no symmetry constrains at the density functional level of theory using the B3LYP. Fig. 5 shows the optimized structure, whereas selected calculated bond lengths and angles concerning the coordination sphere are given in Table 5. Mean experimental bond lengths determined by X-ray structure analysis are also given for comparison. The final optimized structure is a distorted trigonal bipyramidal structure with the nitrogen, the phenolic oxygen and the bromine atom lying in the basal plane with the axial ligand atoms being the carbonyl oxygen and the other nitrogen. An overall agreement has been found between the calculated and experimental structure in each case with the largest deviation of bond distances being about 0.1 Å, while this of bond angles being about 8°. The two rings of benzophenone deviate from planarity by 38° with the experimental value being 59°. This discrepancy is possibly due to crystal packing effects.

In order to explore the potential energy surface (PES) of complex **10** a series of calculations was carried out on a model representative complex namely [Co(salo)(neoc)Br] (salo = salicylaldehyde anion). The starting structures for this full optimization, carried out in the same level of theory, were all possible trigonal bipyramidal (TBP) or square pyramidal (SP) geometries. Furthermore, for each geometry two initial structures were derived by exchanging the two ligating atoms of the salo ligand, that is the phenolic and the carbonyl oxygen atoms. The four optimized structures found are shown in Fig. 5, whereas their relative energy and calculated bond distances and angles are given in Table 5. No minimum or transition state has been located with a square pyramidal structure, as all optimizations led to the TBP structure. The most stable structure **11** located as a minimum is indeed a TBP structure similar to this experimentally isolated complex **10**. The next local minimum **12** located only 0.4 kcal/mol higher in energy has also the bromine and a nitrogen atom in the basal plane of the TBP. The only difference from the global minimum **10** is that the phenolic oxygen occupies the axial position instead of the carbonyl oxygen. The rest two structures that have been located, **13** and **14**, have the bromine atom occupying an axial position of the TBP, the nitrogen atoms in the basal plane and differ from each other only in positions of the oxygen atoms. Both are transition states on the PES of the molecule. Inspection of the normal mode of their single imaginary frequency reveals that **13** and **14**, being 3.6 kcal/mol and 1.8 kcal/mol higher than **11** and **12**, interconnect each minimum to its mirror image structure.

3.4. Spectroscopy

3.4.1. Infrared spectra (IR)

In the spectra of the free 2-hydroxy-phenone ligands the intense bands stemming from the stretching and bending vibrational modes of the phenolic OH around 3200 and 1410 cm^{-1}, respectively, disappear from the spectra of all complexes indicating the ligand deprotonation [38]. Also, the bands originating from the C–O stretching vibrations at 1245–1285 cm^{-1}, in the complexes exhibit positive shifts at 1342–1385 cm^{-1} while their intensity is enhanced appreciably denoting coordination through the carbonyl oxygen of the phenone ligand. The band at ~1660 cm^{-1} attributable to the carbonyl bond ν(C=O) of the free ligand, upon coordination, in the complexes is shifted to lower frequencies at ~1605 cm^{-1} thus denoting the bidentate mono-anionic character of the studied hydroxyl-phenone ligands.

The intense bands at 1596 cm^{-1}, attributable to the stretching vibration of C=N (aromatic bond) are present in all complexes. The band at 730 ± 15 cm^{-1}, ascribed to the rocking vibrations of the pyridyl C–H bonds and the band at 860 ± 10 cm^{-1}, attributable to the deformation vibrations of the pyridyl C–H bonds, disclosed the occurrence of the nitrogenous base (neocuproine) in the studied compounds. The medium to low intensity bands at 550–590 and 512, 421 cm^{-1} are attributed to the coordination bonds (Co–

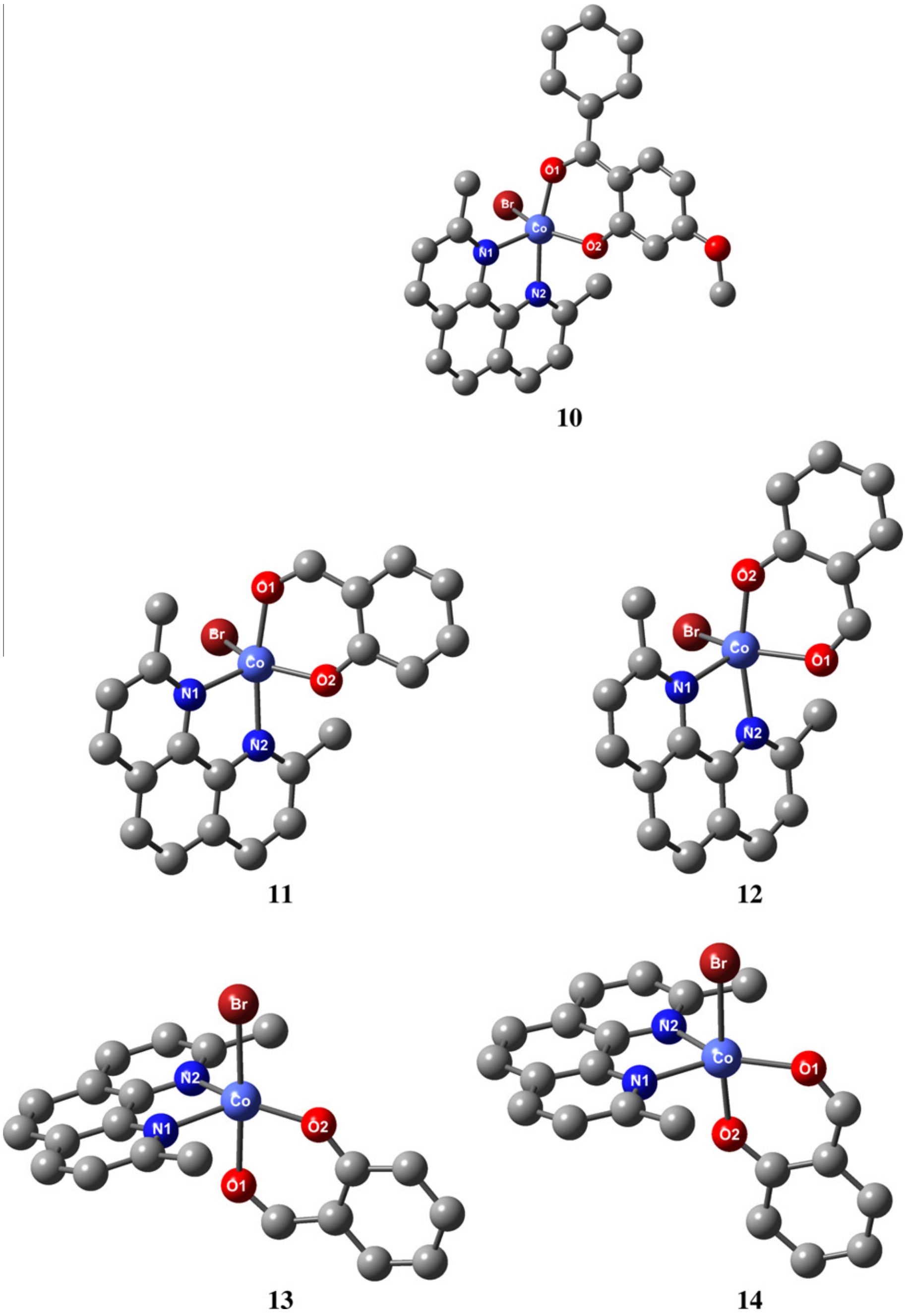

Fig. 5. The isolated complex [Co(opo)(neoc)Br] (**10**), the model [Co(salo)(neoc)Br] (**11**) and its isomers **12**, **13** and **14** (hydrogens not shown for clarity).

O and Co–N, respectively). Thus the medium to low intensity experimental bands located at 420 cm^{-1} and ~560 cm^{-1} for all complexes should be assigned to these Co–N and Co–O vibrations, respectively.

For the [Co(opo)(neoc)Br] (**10**) complex, the observed peaks at 217 and 303 cm^{-1} in the IR spectrum are assigned to Co–Br covalent bond according to the literature [39].

3.4.2. Electronic excitation (UV–Vis) study

Cobalt(II) complexes have electronic spectra which are indicative of their stereochemistry. The experimental absorption spectra (UV–Vis) of the title compounds in acetonitrile solution presented four dominant bands in the region 300–1100 nm (representative spectra are given for compounds **3** and **10** with different geometry in Fig. 6).

In the visible region the first two bands of low energy for the complexes **1**–**5**, are clearly located at 990 nm ($\varepsilon = 20$) and 670 nm ($\varepsilon = 80$), while the expected third one at ~500 nm is not shown, possibly masked due to the neighboring position and the higher ε of the intra-ligand bands. These bands are assigned as d–d excitations and are indicative of an octahedral high-spin Co(II) compound.

The three low energy d–d excitations for the trigonal bipyramidal high-spin Co(II) complexes are expected at 580–600 nm, 510–530 nm and 420–440 nm. The first two bands are clearly located in the experimental spectra of the complexes **6**–**10**, as it is depicted in Fig. 6 for the compound **10** (590 nm ($\varepsilon = 75$), 520 nm ($\varepsilon = 40$)), while the third one is seen as a shoulder at about 420 nm. The appearance of the peaks at 520 nm and 590 nm is typical example of the trigonal bipyramidal geometry around Co(II) [40].

Table 5
Relative energies and selected bond distances (Å) and bond angles (°) calculated for the isolated complex [Co(opo)(neoc)Br] (**10**), the model [Co(salo)(neoc)Br] (**11**) and its isomers **12**, **13** and **14**.[a]

	10	11	12	13	14
Co–O1	2.040 (1.956)[b]	2.063	2.127	2.263	2.089
Co–O2	2.017 (2.081)	2.024	1.989	1.941	2.028
Co–N1	2.138 (2.084)	2.136	2.146	2.099	2.119
Co–N2	2.149 (2.134)	2.150	2.154	2.104	2.119
Co–Br	2.539 (2.594)	2.534	2.533	2.528	2.540
Br–Co–N1	102.9 (108.6)	104.6	105.3	98.1	93.4
Br–Co–O2	141.7 (133.5)	139.9	100.9	100.9	175.5
N1–Co–O2	113.0 (116.9)	113.3	105.1	132.2	89.8
O1–Co–Br	96.8 (89.6)	95.3	138.8	176.1	90.9
O1–Co–N1	107.8 (102.4)	106.9	112.5	80.8	140.6
O1–Co–O2	84.9 (91.5)	86.0	84.8	82.4	84.6
N2–Co–Br	90.5 (96.2)	91.0	91.6	96.7	93.4
N1–Co–N2	78.3 (80.6)	79.0	78.8	81.5	79.5
N2–Co–O2	83.9 (78.2)	84.0	156.2	138.0	90.3
O1–Co–N2	168.6 (169.4)	169.9	80.6	79.5	139.3
DE (kcal/mol)	–	0.0	0.4	2.2	3.6

[a] Numbering scheme as in Fig. 5.

[b] Experimental values in parentheses.

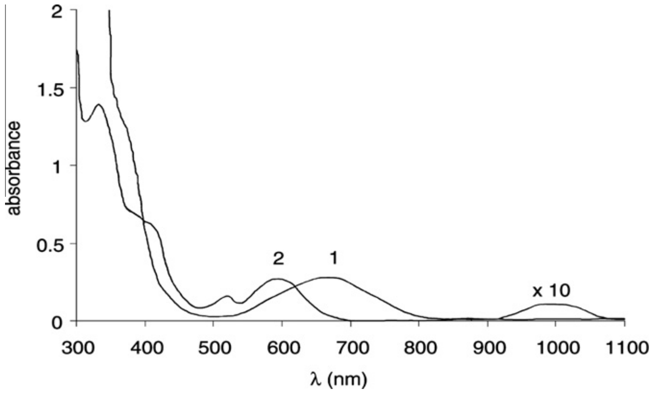

Fig. 6. Electronic absorption spectra (UV–Vis) of the complexes **1**: [Co(bpo)$_2$(neoc)] (**3**) and **2**: [Co(opo)(neoc)Br] (**10**) in C = 10^{-4} M CH$_3$CN.

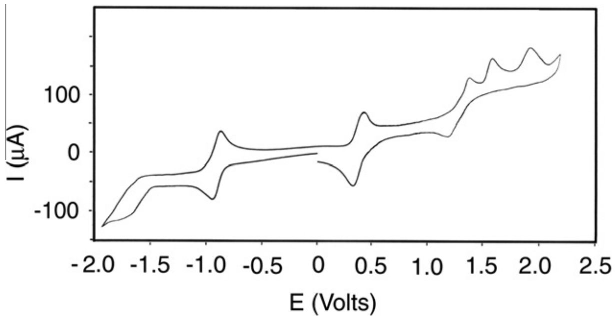

Fig. 7. Cyclic voltammetry diagram of [Co(bpo)$_2$(neoc)] (**3**) in CH$_3$CN (0.1 M TEAP, C = 10^{-3} M, scan rate 100 mV/s).

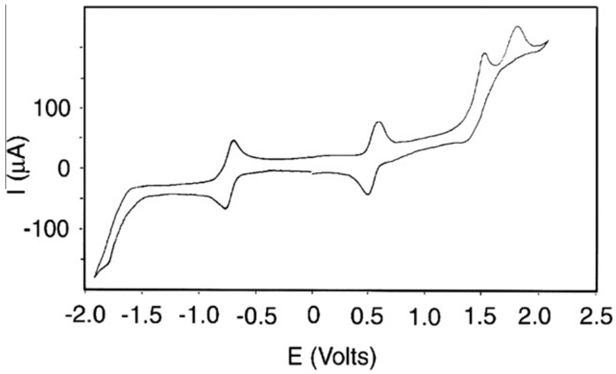

Fig. 8. Cyclic voltammetry diagram of [Co(opo)(neoc)Br] (**10**), in CH$_3$CN (0.1 M TEAP, C = 10^{-3} M, scan rate 100 mV/s).

Finally, the excitations at 310–320 nm and 280–295 nm arising from intra-ligand π–π transitions within the 2-OH-benzophenone and neoc ligands, are seen in the spectra of the complex **10** at 320 (ε = 11000) and 283 (ε = 13000) not shown here), respectively.

3.5. Cyclic voltammetry (CV)

All the studied compounds exhibit similar behavior during the cyclic voltammetry experiments. The typical CV diagrams of compounds **3** and **10** are representatively depicted in Figs. 7 and 8, while the experimental data for the studied compounds are presented in Table 6. The CVs in the region −1950 to 2100 mV for all compounds revealed five redox waves.

Waves I and II exhibited at around −830 and 550 mV represent the single electron redox potentials of the assigned couples Co(I)–Co(II) and Co(II)–Co(III), respectively. Both are reversible and, as compared with the waves observed from equimolar amount of ferrocene under the same experimental conditions, are due to one electron transformations [17,18 and references therein].

Wave III around 1510 mV and wave IV around −1820 mV are assigned to the oxidation and the reduction, respectively, of the phenolic oxygen from the deprotonated 2-OH-phenone ligands in the complexes. In the case of compounds **1**–**5**, both are two electrons wave transformations and this suggests that the deprotonated 2-OH-phenone ligands in the octahedral complexes are equivalent. In the case of compounds **6**–**10** both are one electron transformations as expected. Wave V around 1860 mV and at higher voltage values can be attributed to the oxidation of the nitrogen atoms of the nitrogenous base.

3.6. Thermal studies

The thermal behavior for three of the title compounds, (**3**-belonging to the octahedral addition compounds) and (**9** and **10**-belonging to the trigonal bipyramidal complexes), was studied in nitrogen atmosphere, over the temperature range ambient to 980 °C by using the simultaneous TG/DTG–DTA technique. The studied compounds are unstable upon heating, decomposing in successive stages.

The first sudden mass loss for compound **3**, [Co(bpo)$_2$(neoc)] (Fig. 9) coincides with the mass loss of a benzophenon moiety (PhCO) derived from a bpo ligand, (DTGmax at 305 °C, experimental mass loss 15.3% and theoretical 15.88%). The second sudden mass loss until 550 °C with DTGmax at 368 °C, coincides well with the further mass loss of one bpo ligand (29.7% f. and 29.8% c.). The DTA curve shows one sharp endothermic peak at 254 °C, which is attributed to simultaneous melting and decomposition of the compound, while the next two small endothermic peaks to further decomposition. Upon increasing the temperature, the unstable intermediates undergo further decomposition with gradually mass loss in a wide temperature range (550–980 °C), which is attributed to the remaining organic fragments of the ketone ligand and fragments of the neocuproine. The amount of the solid residue at 980 °C, is much higher than the calculated for the metallic cobalt 8.92% or for the cobalt oxide CoO 11.34%. This suggests that the residue consists from a carbonaceous mixture, resulted from the uncompleted pyrolysis of the compound [34,41].

Table 6
Redox waves of the studied compounds in CH_3CN (0.1 M TEAP, C = 10^{-3} M, scan speed 100 mV/s).

Comp.	Wave I			Wave II			Wave III	Wave IV	Wave V
	E_{pa}	E_{pc}	$E_{1/2}$	E_{pa}	E_{pc}	$E_{1/2}$	E_{pa}	E_{pc}	E_{pa}
1	−0.87	−0.83	−0.85	0.58	0.53	0.56	1.53	−1.83	1.92
2	−0.85	−0.80	−0.82	0.56	0.52	0.54	1.53	−1.84	1.93
3	−0.87	−0.83	−0.85	0.56	0.51	0.53	1.51	−1.81	1.95
4	−0.85	−0.81	−0.83	0.56	0.53	0.55	1.50	−1.82	1.95
5	−0.86	−0.81	−0.84	0.56	0.52	0.54	1.53	−1.84	1.89
6	−0.86	−0.84	−0.85	0.57	0.54	0.56	1.51	−1.82	1.88
7	−0.85	−0.82	−0.83	0.57	0.53	0.55	1.52	−1.82	1.87
8	−0.86	−0.82	−0.84	0.55	0.52	0.53	1.54	−1.84	1.89
9	−0.85	−0.82	−0.84	0.56	0.54	0.55	1.50	−1.80	1.89
10	−0.86	−0.82	−0.84	0.57	0.53	0.55	1.51	−1.82	1.89

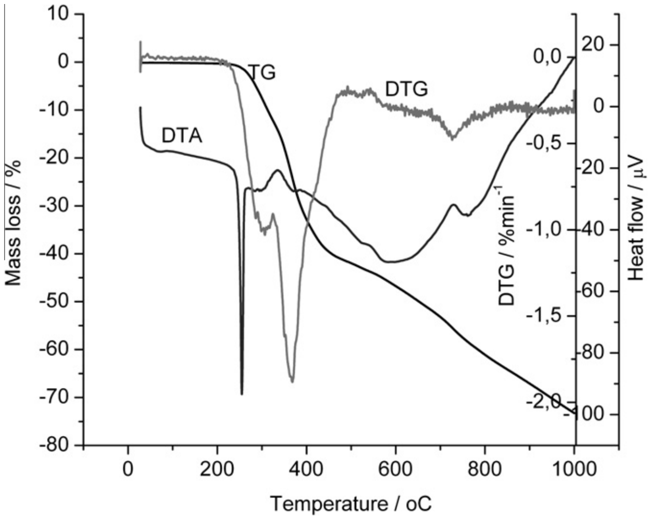

Fig. 9. Thermoanalytical curves (TG, DTG, DTA) for the compound **3**, $[Co(bpo)_2(neoc)]$ with heating rate 5 °C min^{-1} in N_2 atmosphere.

In the trigonal bipyramidal complexes **9**, [Co(bpo)(neoc)Br] and **10**, [Co(opo)(neoc)Br], the thermal decomposition starts with the elimination of the coordinated bromide without melting of the compounds, as it is evident from the DTA curves and continues with the elimination of the organic parts of the ligands. Representatively, for compound **9** (Fig. 10) the sudden mass loss 12.5% found of the first stage (115–215 °C, DTG peak at 188 °C, DTA broad endothermic centered at 384 °C) could be attributed to the elimination of a bromide (calculated 14.70%). The decomposition continues again with sudden mass loss of 30.0% found until 500 °C and successively gradual mass loss until 680 °C (36.0% found for the temperature range 215–680 °C), which coincides with the elimination of one bpo molecule (calculated 36.21%). The existence of a double sharp endothermic peak on the DTA curve at 252 and 274 °C, at the beginning of the second decomposition stage, denotes a possible transformation that could take place after the elimination of the bromide atom.

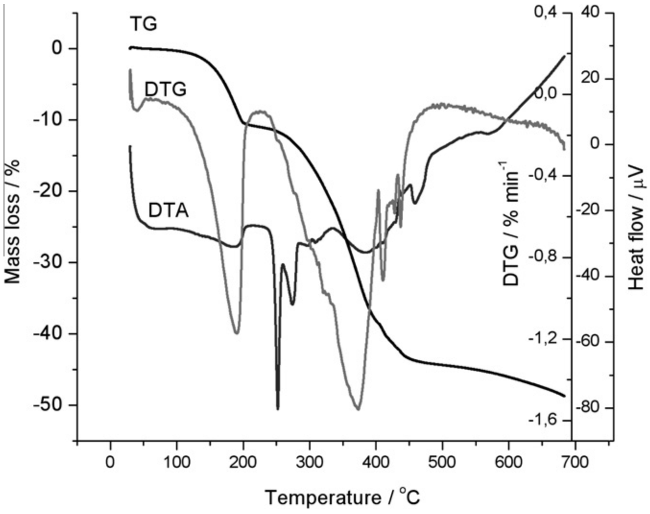

Fig. 10. Thermoanalytical curves (TG, DTG, DTA) for the compound **9**, [Co(bpo)(neoc)Br] with heating rate 5 °C min^{-1} in N_2 atmosphere.

In order to verify the solid residues, as they deduced and estimated from the TG and DTG curves, powder XRD studies were used. It was found that the solid material, at 980 °C consists mainly from cubic metallic cobalt.

4. Conclusions

Five octahedral [Co(2-hydroxy-benzophenone)$_2$(neoc)] and five trigonal bipyramidal [Co(2-hydroxy-benzophenone)(neoc)Br] (ketone = anion of 2-hydroxy-benzophenones) compounds were synthesized and characterized.

The theoretical DFT investigation with GAUSSIAN-03 showed that the most stable structure located as a minimum is indeed a TBP structure similar to this described by the crystal structure for complex [Co(2-hydroxy-4-methoxybenzophenone)(neoc)Br].

X-ray study of the compounds **3**, **10** and **11** verified the existence of mononuclear Co(II) compounds with different geometries around the metal ion.

The cyclic voltammetry study in CH_3CN gave all the expected waves for the redox processes of the metal Co(II) and the studied ligands.

The compounds are stable at ambient temperature, but unstable upon heating decomposing in several stages, giving at 980 °C in nitrogen atmosphere a solid product consisting of carbonaceous metallic cobalt.

Appendix A. Supplementary data

CCDC 707802, 709172, and 803882 contain the supplementary crystallographic data for **3**, **10**, and **11**, respectively. These data can be obtained free of charge via http://www.ccdc.cam.ac.uk/conts/retrieving.html, or from the Cambridge Crystallographic Data Centre, 12 Union Road, Cambridge CB2 1EZ, UK; fax: (+44) 1223-336-033; or e-mail: deposit@ccdc.cam.ac.uk.

References

[1] (a) F. Barigelletti, B. Ventura, J.-P. Collin, R. Kayhanian, P. Gavina, J.-P. Sauvage, Eur. J. Inorg. Chem. (2000) 113;

(b) M.S. Lüth, L.E. Kapinos, B. Song, B. Lippert, H. Sigel, J. Chem. Soc., Dalton Trans. (1999) 357.
[2] G.J. Weijnen, A. Koudijs, J.F. Engbersen, J. Org. Chem. 57 (1992) 7258.
[3] D.S. Siegman, Biochemistry 29 (1990) 9097.
[4] E. Peña-Cabrera, P.-O. Norrby, M. Sjögren, A. Vitagliano, V. De Felice, J. Oslob, S. Ishii, D. O'Neill, B. Åkermark, P. Helquist, J. Am. Chem. Soc. 118 (1996) 4299.
[5] D.J. Szalda, C. Creutz, D. Mahajan, N. Sutin, Inorg. Chem. 22 (1983) 2372.
[6] J. Reedijk, in: G. Wilkinson, R.D. Gillard, J.A. Mc-Cleverty (Eds.), Comprehensive Coordination Chemistry, vol. 2, Pergamon Press, Oxford, UK, 1987, pp. 73–98.
[7] C.M. Taylor, S.P. Watton, P.A. Bryngelson, M.J. Maroney, Inorg. Chem. 42 (2003) 312.
[8] R.N. Prasad, A. Agrawal, J. Ind. Chem. Soc. 83 (2006) 75.
[9] S.T. Hussain, H. Ahmad, M.A. Atta, M. Afzal, M. Saleem, J. Trace Microprobe Tech. 16 (1998) 139.
[10] K. Fujinaga, Y. Sakaguchi, T. Tsuruhara, Y. Seike, M. Okumura, Solvent Extr. Res. Dev. 8 (2001) 144.
[11] P. Sajith, M.T. Ummer, N. Mandal, S.K. Mandot, S.L. Agrawal, S. Bandyopadhyay, R. Mukhopadhyay, B. D'Cruz, A.S. Deuri, P. Kuriakose, J. Adhes. Sci. Technol. 19 (2005) 1475.
[12] (a) Z.-Y. Xiong, Li-J. Liu, Z.-Y. Xiong, L.-J. Liu, Acta Crystallogr., Sect. E 61 (2005) m863;
(b) Q. Chen, Acta Crystallogr., Sect. E 62 (2006) m56.
[13] Y.-X. Sun, G.-Z. Gao, Acta Crystallogr., Sect. E 61 (2005) m354.
[14] Y.-M. Yang, P.-C. Lu, T.-T. Zhu, C.-H. Liu, Acta Crystallogr., Sect. E 63 (2007) m1613.
[15] J.C. Pessoa, I. Cavaco, I. Correia, I. Tomaz, T. Duarte, P.M. Matias, J. Inorg. Biochem. 80 (2000) 35.
[16] M. Lalia-Kantouri, T. Dimitriadis, C.D. Papadopoulos, M. Gdaniec, A. Czapik, A.G. Hatzidimitriou, Z. Anorg. Allg. Chem. 635 (2009) 2185.
[17] C.D. Papadopoulos, A.G. Hatzidimitriou, G.P. Voutsas, M. Lalia-Kantouri, Polyhedron 26 (2007) 1077.
[18] C.D. Papadopoulos, M. Lalia-Kantouri, J. Jaud, A.G. Hatzidimitriou, Inorg. Chim. Acta 360 (2007) 3581.
[19] C.D. Papadopoulos, A.G. Hatzidimitriou, M. Quiros, M.P. Sigalas, M. Lalia-Kantouri, Polyhedron 30 (2011) 486.
[20] A.D. Becke, J. Chem. Phys. 98 (1993) 5648.
[21] K.Y. Lee, W. Yang, R.G. Parr, Phys. Rev. B37 (1988) 785.
[22] P.J. Hay, W.R. Wadt, J. Chem. Phys. 82 (1985) 270.
[23] W.R. Wadt, P.J. Hay, J. Chem. Phys. 82 (1985) 284.
[24] P.J. Hay, W.R. Wadt, J. Chem. Phys. 82 (1985) 299.
[25] T.H. Dunning Jr., P.J. Hay, in: H.F. Schaefer (Ed.), Modern Theoretical Chemistry, vol. 3, third ed., Plenum Press, New York, 1977, pp. 1–28. Chapter 1.
[26] M.J. Frisch, G.W. Trucks, H.B. Schlegel, G.E. Scuseria, M.A. Robb, J.R. Cheeseman, V.G. Zakrzewski, J.A. Montgomery, R.E. Stratmann, J.C. Burant, S. Dapprich, J.M. Millam, A.D. Daniels, K.N. Kudin, M.C. Strain, O. Farkas, J. Tomasi, V. Barone, M. Cossi, R. Cammi, B. Mennucci, C. Pomelli, C. Adamo, S. Clifford, J. Ochterski, G.A. Petersson, P.Y. Ayala, Q. Cui, K. Morokuma, P. Salvador, J.J. Dannenberg, D.K. Malick, A.D. Rabuck, K. Raghavachari, J.B. Foresman, J. Cioslowski, J.V. Ortiz, A.G. Baboul, B.B. Stefanov, G. Liu, A. Liashenko, P. Piskorz, I. Komaroni, R. Gomperts, R.L. Martin, D.J. Fox, T. Keith, M.A. Al-Laham, C.Y. Peng, A. Nanayakkara, M. Challacombe, P.M.W. Gill, B. Johnson, W. Chen, M.W. Wong, J.L. Andres, C. Gonzalez, M. Head-Gordon, E.S. Replogle, J.A. Pople, Gaussian 03, Gaussian, Inc., Pittsburgh, PA, 2003.
[27] L. Palatinus, G. Chapuis, J. Appl. Crystallogr. 40 (2003) 786.
[28] (a) G.M. Sheldrick, Acta Crystallogr., Sect. A 64 (2008) 112;
(b) G.M. Sheldrick, SHELX-97, Program for Crystal Structures Refinement, University of Gottingen, Gottingen, Germany, 1997.
[29] P.W. Betteridge, J.R. Carruthers, R.I. Cooper, K. Prout, D.J. Watkin, J. Appl. Crystallogr. 36 (2003) 1487. Program CRYSTALS, Ver. 12.83 and 12.86.
[30] Th. Kramer, J. Strahle, Z. Naturforsch. B 41 (1986) 692.
[31] F.A. Cotton, G. Wilkinson, Advanced Inorganic Chemistry, John Wiley, NY, 1988. p. 730.
[32] K.N. Patel, N.H. Patel, K.M. Patel, M.N. Patel, Synth. React. Inorg. Met.-Org. Chem. 30 (2000) 921.
[33] D.J. Walker, C.K. Prout, F.J. Bearch, CAMERON Program, Chemical Crystallographic Laboratory, Oxford University, UK, 1996.
[34] M. Lalia-Kantouri, M. Gdaniec, A. Czapik, K. Chrissafis, W. Ferenc, J. Sarzynski, Ch.D. Papadopoulos, J. Therm. Anal. Calorim. (2012), http://dx.doi.org/10.1007/s10973-011-1692-5.
[35] (a) A.K. Patra, M. Ray, R. Mukherjee, J. Chem. Soc., Dalton Trans. (1999) 2461;
(b) C.E. Searls, S.T. Kleespies, M.L. Eppright, S.C. Schwartz, G.P. Yap, R.C. Scarrow, Inorg. Chem. 49 (2010) 11261.
[36] A.W. Addison, T.R. Nagaswara, J. Reedijk, J. Van Rijn, G.C. Verschoor, J. Chem. Soc., Dalton Trans. (1984) 1349.
[37] V.M. Leovac, Z.D. Tomic, K.M. Szecsenyi, L.S. Jovanovic, M.D. Joksovic, J. Serb. Chem. Soc. 72 (2007) 1281.
[38] R.M. Silverstein, G.C. Bassler, G. Morvill, Spectrometric Identification of Organic Compounds, sixth ed., Wiley, New York, 1998. p. 87.
[39] K. Nakamoto, Infrared and Raman Spectra of Inorganic and Coordination Compounds, fifth ed., Wiley-Interscience, New York, 1997.
[40] A.B. Lever, Inorganic Electronic Spectroscopy, second ed., Elsevier, 1984. p. 480.
[41] W. Ferenc, B. Cristvao, J. Sarzynski, J. Therm. Anal. 101 (2010) 761.